Bridging the Last Mile of Prediction: Enhancing Time Series Forecasting with Conditional Guided Flow Matching

Huibo Xu¹ Runlong Yu² Likang Wu³ Xianquan Wang¹ Qi Liu^{1*}

¹University of Science and Technology of China ²University of Pittsburgh ³Tianjin University

Abstract

Existing generative models for time series forecasting often transform simple priors (typically Gaussian) into complex data distributions. However, their sampling initialization, independent of historical data, hinders the capture of temporal dependencies, limiting predictive accuracy. They also treat residuals merely as optimization targets, ignoring that residuals often exhibit meaningful patterns like systematic biases or nontrivial distributional structures. To address these, we propose Conditional Guided Flow Matching (CGFM), a novel model-agnostic framework that extends flow matching by integrating outputs from an auxiliary predictive model. This enables learning from the probabilistic structure of prediction residuals, leveraging the auxiliary model's prediction distribution as a source to reduce learning difficulty and refine forecasts. CGFM incorporates historical data as both conditions and guidance, uses two-sided conditional paths (with source and target conditioned on the same history), and employs affine paths to expand the path space, avoiding path crossing without complex mechanisms, preserving temporal consistency, and strengthening distribution alignment. Experiments across datasets and baselines show CGFM consistently outperforms state-of-the-art models, advancing forecasting.

Introduction

Time series forecasting, a fundamental task in time series analysis, is widely used and has a considerable impact in various domains such as finance, healthcare, and energy (Lim and Zohren 2021). Traditionally viewed as the process of predicting future values from historical observations, it can also be framed as a conditional generation problem, where future data are generated conditioned on history data (Shen and Kwok 2023). Naturally, Generative models have thus emerged as powerful tools for this task (Li et al. 2022; Yoon, Jarrett, and Van der Schaar 2019), with diffusion models achieving success for their predictive distribution modeling capabilities and conditional generation mechanisms, achieving notable success in time series forecasting (Kollovieh et al. 2024a).

Currently, most generative models for time series forecasting transform a simple prior, typically Gaussian, into a complex data distribution, often under rigid generation constraints. However, because sampling is initialized independently of historical data, these models struggle to capture

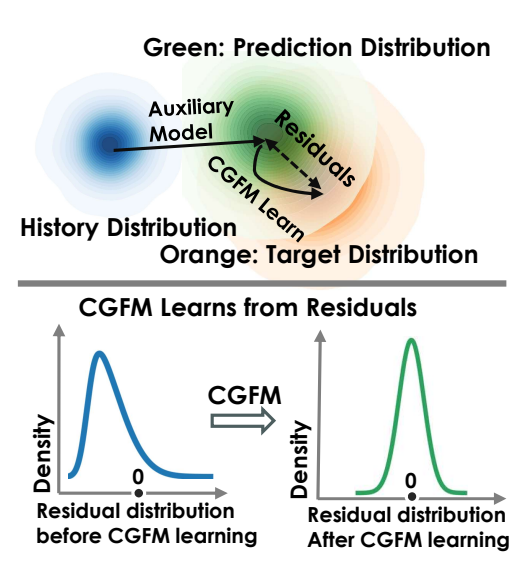


Figure 1: Top: Auxiliary models learn a prediction distribution that differs from the target, leading to residuals. CGFM learns the probabilistic structure of these residuals. Bottom: CGFM reduces the residuals to be centered and concentrated around zero (mean tending to zero with significantly reduced variance).

temporal dependencies, which in turn limits predictive accuracy. In addition, forecasting models typically treat residuals purely as optimization targets, minimizing them through loss functions without modeling them as structured, learnable signals. Yet in practice, residuals often exhibit meaningful patterns, such as systematic biases or nontrivial distributional structures. Modeling these residuals, rather than discarding them after optimization, represents a promising direction for enhancing forecasting performance.

To address these challenges, we turn to flow matching (Esser et al. 2024; Kerrigan, Migliorini, and Smyth 2023; Lipman et al. 2023), a state-of-the-art generative modeling framework that offers greater flexibility in both the choice of initial distributions and the design of sampling trajectories, while also producing higher-quality results compared to diffusion models. Leveraging these advantages, we propose Conditional Guided Flow Matching (CGFM), a novel fore-

^{*}Corresponding author: qiliuql@ustc.edu.cn

casting framework designed to enhance predictive accuracy by learning the probabilistic structure of residuals between model predictions and true future values, thereby refining predictions toward the target distribution.

First, we utilize the distribution of an auxiliary model's predictions as the source distribution, rather than constraining it to a simple noise distribution. On one hand, the prediction distribution of the auxiliary model preserves richer temporal dependencies compared to a Gaussian prior and serves as the closest accessible approximation to the target distribution, naturally reducing the learning difficulty when starting from a distribution closer to the target. On the other hand, as we will demonstrate later, this flow matching formulation is equivalent to learning the probabilistic characteristics of the residuals, going beyond merely minimizing loss functions. By exploiting the valuable information encoded in the prediction residuals, our approach further refines the results and achieves improved forecasting accuracy.

Second, the essence of forecasting lies in capturing the relationship between historical data and future target values. We innovatively incorporate historical data into both probability path construction and velocity field learning. Key innovations include a two-sided conditional probability path, in which both the source and target distributions are conditioned on the same historical data, as a generalization of linear ones. This two-sided design, together with our choice of source distribution, model structure, and the flexibility of affine paths, theoretically guarantees the avoidance of path crossing, a critical challenge in flow-based modeling, without relying on complex restrictive mechanisms such as OT-CFM's (Tong et al. 2024) optimal transport plans or Rectified Flow's (Liu, Gong, and Liu 2022) specialized training schemes. Affine paths expand the space of probability paths, enabling more flexible adaptation to varying initial distributions. By preventing path crossing, the framework reduces prediction ambiguity and information loss during sampling, which contributes to improved forecasting performance. Historical data guides the velocity field to effectively capture temporal dependencies, further strengthening the alignment between source and target distributions. Additionally, reparameterizing the prediction target to directly optimize toward the target data further enhances accuracy.

Our main contributions are as follows:

- We propose a novel model-agnostic time series forecasting framework, extending flow matching by integrating the outputs of an auxiliary model. This enables learning from prediction residuals, leveraging the auxiliary model's prediction distribution as a source to reduce learning difficulty and refine forecasts
- We innovatively integrate historical data as two-sided conditions into both probability path construction and velocity field learning: by designing two-sided conditional probability paths and combining general affine paths, we naturally avoid path crossing without relying on complex restrictive mechanisms. This design inherently fits the temporal dependencies of time series data, preserves temporal consistency, and strengthens distribution alignment, thereby boosting accuracy.

 We conduct extensive experiments, demonstrating that CGFM consistently improves forecasting performance and outperforms state-of-the-art models, validating its effectiveness and generality.

Preliminaries

Flow Matching

Given a sample X_0 drawn from a source distribution p such that $X_0 \sim p$, in d-dimensional Euclidean space where $X_0 = (x_0^1, \dots, x_0^d) \in \mathbb{R}^d$, and a target sample $X_1 = (x_1^1, \dots, x_1^d)$ $X_1 \sim q$. Flow Matching (FM) constructs a probability path $(p_t)_{0 \leq t \leq 1}$ from the known distribution $p_0 = p$ to the target distribution $p_1 = q$, where p_t is a distribution over \mathbb{R}^d . Specifically, Flow Matching employs a straightforward regression objective to train the velocity field neural network, which describes the instantaneous velocities of samples. The relationship between the velocity field and the flow is defined as:

$$\frac{d}{dt}\psi_t(x) = u_t(\psi_t(x)),\tag{1}$$

where $\psi_t(x)$ represents the flow at time t, and $\psi_0(x) = x$. The velocity field u_t generates the probability path p_t if its flow ψ_t satisfies $X_t := \psi_t(X_0) \sim p_t$ for $X_0 \sim p_0$. The goal of Flow Matching is to learn a vector field $u_\theta(t)$ such that its flow ψ_t generates a probability path p_t with $p_0 = p$ and $p_1 = q$. The Flow Matching loss is defined as: $\mathcal{L}_{\text{FM}}(\theta) = \mathbb{E}_{t,X_t} \left[\left\| u_t(X_t) - u_t^\theta(X_t) \right\|^2 \right],$

Related Work

We present the most relevant related work here. Additional references are provided in the appendix.

Flow Matching for Time Series

Flow Matching (FM) has received increasing attention in time series modeling for its efficiency in constructing continuous probability paths via velocity fields. Early work such as CFM-TS (Tamir et al. 2024) explored FM for time series generation using Brownian bridges and Gaussian processes, offering improved stability over neural ODEs. TSFlow (Kollovieh et al. 2024b) further addressed the large distributional gap between source and target by coupling GP-informed priors with optimal transport, though it only incorporated historical data during inference, limiting its temporal modeling capacity during training. FM-TS (Hu et al. 2024) applied rectified flows in a basic form, demonstrating applicability but lacking structured conditioning. TFM (Zhang et al. 2024) focused on clinical forecasting with memory-based trajectory coupling for irregular sampling and covariates but is limited by historical window constraints and general priors, underutilizing complex temporal dependencies and structured signals. CGFM's bilateral conditional design—with non-crossing paths, residual learning, and model independence—advances temporal consistency, efficiency, and flexibility for time series forecasting. Despite progress, existing methods suffer from weak historical data use and over-reliance on generic priors. Our CGFM addresses this via an auxiliary model's predictive distribution (more target-closer than GP priors) to correct residuals, plus

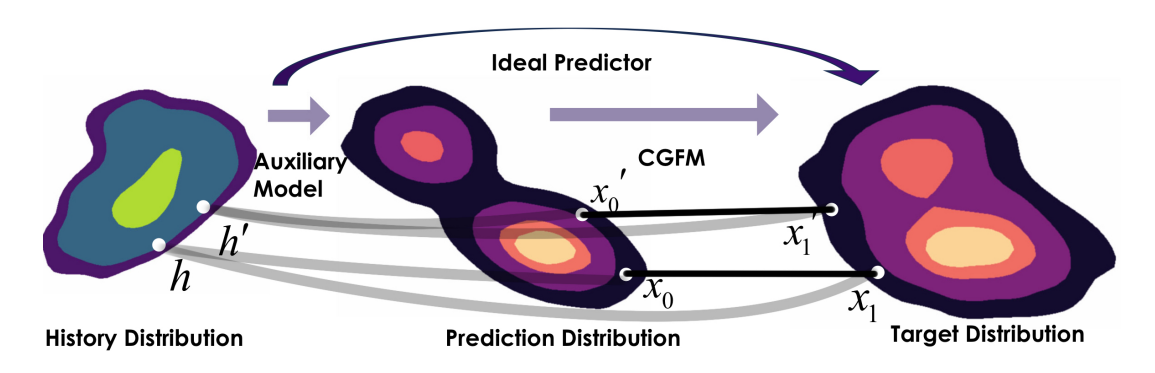


Figure 2: Visualization of CGFM training. The ideal predictor maps the history distribution to the target distribution. However, in practice, the prediction distribution of the auxiliary model inevitably deviates from the target distribution. CGFM enhances prediction by learning the path between the prediction and target distributions. The black line between x_0 and x_1 represents the two-sided conditional guided probability path, while h generates x_0 and x_1 along the gray line, facilitating the learning of this path.

two-sided conditional paths (historical-guided) for consistency and non-crossing; with affine interpolation, it captures residual dynamics and boosts accuracy.

CGFM

In time series prediction tasks, the goal is to leverage historical data to predict future data. Let $H \in \mathbb{R}^{C \times L} \sim p_H$ denote the historical data, with samples represented by h. Similarly, let $F \in \mathbb{R}^{C \times F} \sim q$ represent the target future data, with samples denoted by f. The probability path is defined as p_t , where $X_t \sim p_t$ represents the state of the data at time t. The objective is to predict the future data F, where in the flow matching framework, q serves as the target distribution. Specifically, at $t = 1, X_1 \in \mathbb{R}^{C \times F} \sim q$, with samples denoted by x_1 . At t=0, the source data is given by $X_0 \in \mathbb{R}^{C \times F} \sim p$, with samples represented by x_0 .

Choice of X_0

To fully leverage the valuable information encoded in the predictions residuals, we harness the flexibility of flow matching by setting X_0 as the output generated by a predictive auxiliary model, i.e., $X_0 = X_{\text{aux}} = \Phi(H)$. In this case, the distribution p conditioned on h can be expressed as $p(x_0 \mid h)$, representing the distribution of the auxiliary model's predictions. Specifically, we design a probability path that from the distribution of the auxiliary model's predictions to the target distribution. This allows flow matching to effectively learn from prediction residuals of the auxiliary model.

Analysis of the $p(x_0 \mid h)$ Distribution

Since time series datasets are typically stored with a limited number of significant digits and consist of a finite number of samples, even if the original time series is continuous, Hcan only be considered to have an approximately continuous distribution in $\mathbb{R}^{C \times L}$. In general, most models are differentiable, and thus $\Phi(H)$ can also be approximated as $C(\mathbb{R}^{C\times F})$. However, this is insufficient to ensure that $p(x_0 \mid h)$ is C^1 in $\mathbb{R}^{C \times L}$

Proposition 0.1 (Noise Smoothing). Let $X \in \mathbb{R}^{C \times F}$ be a time series with distribution P_{ori} . Define the perturbed series R as: $R = X + \sigma \epsilon$, where $\epsilon \sim \mathcal{N}(0, I)$ is additive Gaussian noise and $\sigma > 0$. The perturbed series R follows the distribution P_{per} :

$$P_{per}(r) = \int P_X(r - \sigma \epsilon) P_{\epsilon}(\epsilon) d\epsilon, \qquad (2)$$

which belongs to $C^1(\mathbb{R}^d)$. Furthermore, P_{per} has a strictly

positive density and possesses finite second moments. Intuitively, $P_{\rm per}$ can be regarded as the convolution of the original distribution $P_X(x)$ with a Gaussian distribution $P_{\epsilon}(\epsilon)$. Since the Gaussian distribution is a C^{∞} function, $P_R(r)$ is thus not only C^1 but also C^{∞} . When $\Phi(H) + \sigma \epsilon$ is applied, the convolution with Gaussian noise significantly enhances the smoothness of the distribution, eliminating sharp variations and discontinuities present in the original distribution. This process ensures that the source remains a valid density while promoting diversity, aligning the noise-smoothed source distribution p with Proposition 0.4, which will be discussed later.

Two-Sided Conditional Guided Prediction

For flow matching where the initial distribution is set to the predictions of the auxiliary model, the target distribution qused during training is derived from the inherent correspondence between future data F and historical data H in the dataset, which can be formulated as $q(x_1 \mid h)$.

The next step is to learn the probability path from $p(x_0 \mid h)$ to $q(x_1 \mid h)$. For time series forecasting tasks, which fundamentally involve learning the mapping from historical sequences to target sequences, a natural and reasonable approach is to incorporate h as conditional guidance into the velocity field u_t . Consequently, the probability path is also conditioned on h.

Accordingly, our goal is to learn a probability path $p_{t|H}(x|h)$ and a velocity field $u_t(x|h)$, ensuring that $u_t(x|h)$ generates $p_{t|H}(x|h)$. To achieve this, since the transition path between distributions cannot be directly learned, we perform marginalization over the path.

In time series forecasting tasks, for a given h, there exists a correspondence between the samples of the source distribution and the target distribution. Relying solely on one-sided conditioning, as in previous flow matching methods, is therefore inadequate. To address this, we propose two-sided conditionally guided probability paths, where a marginalization probability path is constructed and integrated to obtain $p_{t|H}(x|h)$:

$$p_{t|H}(x|h) = \int p_{t|0,1,H}(x|x_0, x_1, h) \pi_{0,1|H}(x_0, x_1|h) dx_0 dx_1.$$
(3)

Here, $\pi_{0,1|H}(x_0, x_1 \mid h) = q(x_1 \mid h)p(x_0 \mid h)$, indicating that x_0 and x_1 are independent given h, a concept referred to as conditional independent coupling. Both are related to the historical data h.

The two-sided conditionally guided probability path is required to comply with the boundary constraints $p_{0|0,1}(x|x_0,x_1,h)=\delta_{x_0}(x)$ and $p_{1|0,1}(x|x_0,x_1,h)=\delta_{x_1}(x)$. Here, δ denotes the Dirac delta function. Subsequently, the velocity field can be obtained as:

$$u_t(x|h) = \int u_t(x|x_0, x_1, h) p_{0,1|t,H}(x_0, x_1|x, h) dx_0 dx_1, \quad (4)$$

By Bayes' Rule, it follows that:

$$p_{0,1|t,H}(x_0,x_1|x,h) = \frac{p_{t|0,1,H}(x|x_0,x_1,h)\pi_{0,1|H}(x_0,x_1|h)}{p_{t|H}(x|h)}.$$
(5)

Thus, the model learns $u_t(x|x_0,x_1,h)$ to obtain $u_t(x|h)$. According to Eq.(1), $u_t(x|x_0,x_1,h)$ determines $p_{0.1|t,H}(x_0,x_1|x,h)$, and vice versa.

Proposition 0.2 (Equivalence of CGFM and Learning Residual Distribution via Flow Matching). *Under Proposition 0.1 (noise smoothing) and two-sided coupling* $\pi_{0,1|H} = p(x_0|h)q(x_1|h)$, CGFM equivalently learns residual $\epsilon = x_1 - x_0$'s probabilistic characteristics via Flow Matching, with its path and loss tied to ϵ 's evolution.

This equivalence highlights a critical advantage of CGFM: instead of treating residuals merely as errors to be minimized through loss functions, it explicitly models the probabilistic structure of these residuals via flow matching. By tying the learning process to the evolution of $\epsilon = x_1 - x_0$, CGFM leverages the auxiliary model's predictions x_0 —which already encode partial temporal information—as a structured starting point, enabling more efficient learning of how to correct these predictions toward the true future values x_1 .

Velocity Field of Marginal Probability Paths

Previous studies have primarily focused on the application of conditional optimal transport flows. In the scenario of a two-sided condition, this can be formulated as: $X_t \sim p_{t|0,1,H} = tX_1 + (1-t)X_0$. Conditional optimal transport flows addresses the problem of kinetic energy minimization through the optimization formulation: $\arg\min_{p_t,u_t}\int_0^1\int_Z\|u_t(x)\|^2p_t(x)\,dx\,dt$, providing a principled approach to solving such problems. However, in timeseries forecasting, this may not identify the optimal predictive path, particularly when the initial distribution is highly complex. Notably, conditional optimal transport can be regarded

as a special case within the broader family of affine conditional flows (Albergo and Vanden-Eijnden 2023).

$$X_t \sim p_{t|0,1,H} = \alpha_t X_1 + \beta_t X_0,$$
 (6)

where α_t and $\beta_t: [0,1] \to [0,1]$ are smooth functions, satisfying $\alpha_0 = \beta_1 = 0$ and $\alpha_1 = \beta_0 = 1$, with $\dot{\alpha}_t > 0$, and $-\dot{\beta}_t' > 0$ for $t \in (0,1)$. Referring to Eq.(1), let $x' = \psi_t(x)$, and the inverse function yields $\psi_t^{-1}(x') = x$. Consequently, Eq.(1) can be reformulated as

$$u_t(x') = \dot{\psi}_t(\psi_t^{-1}(x')).$$
 (7)

Proposition 0.3 (Velocity Field of Marginal Probability Paths). Under mild assumptions, if $\psi_t(\cdot|x_0,x_1,h)$ is smooth in t and forms a diffeomorphism in x_0,x_1 , then the velocity field $u_t(x)$ can be represented as

field $u_t(x)$ can be represented as $u_t(x|h) = \mathbb{E}\left[\dot{\psi}_t(X_0, X_1|H)|X_t = x, H = h\right] \qquad (8)$ for all $t \in [0, 1)$.

According to Proposition 0.3, under the two-sided condition, the velocity field takes the form of:

$$u_t(x|h) = \mathbb{E}\left[\dot{\alpha}_t X_1 + \dot{\beta}_t X_0 \mid X_t = x, H = h\right].$$
 (9)
The choice of α_t and β_t enhances flexibility, making it better

The choice of α_t and β_t enhances flexibility, making it better suited for complex source distributions and more effective for predictive path construction. We further investigate the effects of different parameterizations of α_t and β_t in Experiment .

Marginalization

After deriving the conditional velocity field $u_t(x|h)$ and the conditional probability path $p_{t|H}(x|h)$ from the marginal velocity field, we must also ensure that $u_t(x|h)$ indeed generates $p_{t|H}(x|h)$.

Proposition 0.4 (Marginalization via Conditional Affine Flows). Under mild assumptions, q has a bounded support and p is $C^1(\mathbb{R}^d)$ with a strictly positive density and finite second moments. These two are related by the conditional independent coupling $\pi_{0,1|H}(x_0,x_1|h) = p(x_0|h)q(x_1|h)$. $p_t(x|h)$ is defined as Eq.(3), with ψ_t defined by Eq.(6). Subsequently, the marginal velocity engenders p_t that interpolates between p and q.

According to Proposition 0.1, whether p represents the noise distribution or the output distribution of the auxiliary model, appropriate operations can ensure that the C^1 condition is satisfied. Consequently, Proposition 0.4 guarantees the correctness of the flow matching construction.

Proposition 0.5 (Transportation and Non-crossing of Probability Paths). Under the assumptions of Proposition 0.4, further suppose that the affine conditional path and the velocity field are given by Eq. (6) and Eq. (9), respectively. Then All paths of the flow are non-crossing: there exist no $t \in [0,1)$, $z \in \mathbb{R}^d$, and distinct initial conditions $X_0^{(1)} \neq X_0^{(2)}$ such that $X_t^{(1)} = X_t^{(2)} = z$ with distinct evolution directions.

As visualized in Figure 3, this guarantee of non-crossing paths is critical for time series forecasting, as path crossing would lead to ambiguous mappings between the auxiliary model's predictions x_0 and the true future values x_1 at intermediate time steps t. Such ambiguity could cause information loss or conflicting signals during the flow's evolution, undermining the model's ability to refine predictions consistently.

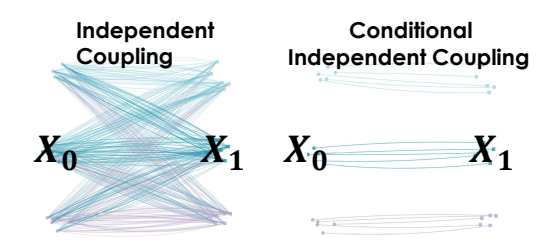


Figure 3: Illustration of Proposition 0.5. Left: Independent coupling may produce crossing paths. Right: CGFM's conditional independent coupling ensures non-crossing paths by conditioning both source and target on shared history

Parameterization of the Prediction Target

Numerous studies in the domains of time-series forecasting and protein synthesis(Watson et al. 2023; Shen, Chen, and Kwok 2024; Shen and Kwok 2023), have undertaken the reparameterization of prediction targets.

In the case of our two-sided condition's affine path By using Eq.(6), we obtain:

$$X_{1} = \frac{X_{t} - \beta_{t} X_{0}}{\alpha_{t}}, X_{0} = \frac{X_{t} - \alpha_{t} X_{1}}{\beta_{t}}.$$
 (10)

Substituting Eq.(10) into Eq.(9) allows for the following reparameterization:

$$u_t(x|h) = \dot{\alpha}_t E[X_1|X_t = x, h] + \dot{\beta}_t E[X_0|X_t = x, h]$$
 (11)

$$= \frac{\dot{\beta}_t}{\beta_t} x + \left[\dot{\alpha}_t - \frac{\alpha_t \dot{\beta}_t}{\beta_t} \right] E[X_1 | X_t = x, H = h]$$
 (12)

$$= \frac{\dot{\alpha}_t}{\alpha_t} x + \left[\dot{\beta}_t - \frac{\beta_t \dot{\alpha}_t}{\alpha_t} \right] E[X_0 | X_t = x, H = h]. \tag{13}$$

Whereas Eq.(12) provides a parameterization of u_t for predicting the target x_1 , where $x_{1|t}(x) = \mathbb{E}[X_1|X_t = x]$ is defined as the x_1 -prediction. Eq.(13) offers a parameterization of u_t for the source x_0 , where $x_{0|t}(x) = \mathbb{E}[X_0|X_t = x]$ is defined as the x_0 -prediction. These equations introduce two novel methods of parameterization. In light of pertinent literature (Watson et al. 2023) and experimental observations, we discern that for sequence prediction tasks, considering our generation target x_1 as our training objective engenders enhanced outcomes.

Loss Function

After obtaining the conditional guided probability path $p_{t|H}(x|h)$ and the velocity field $u_t(x|h)$, we proceed to define the loss function, specifically the guided flow matching loss:

$$\mathcal{L}_{GM}(\theta) = \mathbb{E}_{t,H,X_t} \left[\left\| u_t(X_t \mid H) - u_t^{\theta}(X_t \mid H) \right\|^2 \right], \tag{14}$$

where the velocity field $u_t(X_t \mid H)$ is defined by: $u_t(X_t \mid H) = \mathbb{E}\left[g_t(X_0, X_1) \mid X_t = x, H = h\right]$.

The prediction function $g_t(X_0, X_1)$ is specified based on the prediction target as follows:

$$g_t(X_0, X_1) = \begin{cases} \dot{\alpha}_t X_1 + \dot{\beta}_t X_0, & u_t\text{-Prediction,} \\ X_0, & X_0\text{-Prediction,} \\ X_1, & X_1\text{-Prediction.} \end{cases}$$
(15)

From Eq.(11), Eq.(12), and Eq.(13), it can be shown that the above three prediction methods are mathematically equivalent. If the prediction objective is X_1 -prediction, then after training the velocity field u_t^θ to predict X_1 , it can be substituted into Eq. 12 to replace $\mathbb{E}[X_1 \mid X_t = x, H = h]$, resulting in the velocity field at time t. The same principle applies to x_0 . Furthermore, the conditional guided flow matching loss function $\mathcal{L}_{CGM}(\theta)$ is defined as:

$$\mathcal{L}_{CGM}(\theta) = \mathbb{E}_{t,H,(X_0,X_1) \sim \pi_{0,1|H}} \left[\left\| g_t(X_0, X_1) - u_t^{\theta}(X_t) \right\|^2 \right].$$
(16)

Since $g_t(X_0, X_1)$ is explicitly specified and computable, the loss $\mathcal{L}_{CGM}(\theta)$ offers significant advantages for optimization.

Proposition 0.6. The gradients of the guided flow matching loss and the conditional guided flow matching loss coincide:

$$\nabla_{\theta} \mathcal{L}_{GM}(\theta) = \nabla_{\theta} \mathcal{L}_{CGM}(\theta). \tag{17}$$

Moreover, the minimizer of the Conditional Guided Flow Matching loss $\mathcal{L}_{CGM}(\theta)$ is the marginal velocity $u_t(X_t \mid H)$. **Experiment**

A detailed ablation study, along with detailed explanations of Figure 4 and Figure 5, as well as experimental details such as hyperparameters and additional experiments, can be found in the Appendix.

Experiment Settings

Baseline and Datasets To demonstrate the superiority of our proposed model, CGFM, we compared it against several representative baselines. Among transformer-based models, we included multipatchformer (Naghashi, Boukadoum, and Diallo 2025), iTransformer (Liu et al. 2024), PatchTST (Nie et al. 2023), pathformer (Chen et al. 2024), Autoformer (Chen et al. 2021), and the classic FedFormer (Zhou et al. 2022). Additionally, we incorporated MLP-based models, including RLinear (Li et al. 2023), TimesNet (Wu et al. 2022), Timemixer (Wang et al. 2024) and TiDE (Das et al. 2024). Furthermore, diffusion-based models such as CSDI (Tashiro et al. 2021) and TimeDiff (Shen and Kwok 2023) were also evaluated. Descriptions of the datasets and their statistical properties are detailed in the Appendix.

Evaluation Metrics The experiments employed Mean Squared Error (MSE) and Mean Absolute Error (MAE) to evaluate the predictive performance of the models. To ensure the robustness of the results, each experiment was repeated 10 times, and the outcomes were averaged.

Table 1: Forecasting errors under the multivariate setting. The **bold** values indicate better performance.

Methods Metric		+ CGF E MSE M	FM iTrans MAE MSE	former MAE				Diff MAE		GFM MAE	Multil MSE			GFM MAE
96 E 192 336 720	0.396 0.39 0.428 0.41	05 0.341 0 16 0.372 0	0.336 0.382 0.387 0.427 0.493	$0.392 \\ 0.422$	0.366 0.398	$0.38\overline{2} \\ 0.412$	0.372 0.403	$0.38\overline{1} \\ 0.401$	0.346 0.384	0.389 0.409	0.367 0.399	0.369 0.398	0.339 0.373	0.355 0.378 0.401 0.430
720 96 192 336 720	0.246 0.30 0.310 0.34	05 0.228 0 14 0.281 0	.253 0.179 .298 0.244 .323 0.314 .367 0.413	$0.306 \\ 0.351$	0.242 0.291	0.299 0.329	$0.251 \\ 0.311$	$0.310 \\ 0.352$	0.234 0.283	0.286 0.315	$0.238 \\ 0.305$	0.296 0.342	0.229 0.283	0.255 0.296 0.320 0.371
E 192 336	0.439 0.42 0.480 0.44	24 0.409 0 48 0.425 0	.372 0.389 .417 0.443 .430 0.489 .457 0.506	$0.441 \\ 0.461$	$0.410 \\ 0.428$	0.423 0.437	$0.437 \\ 0.475$	0.429 0.449	0.415 0.423	0.421 0.432	$0.434 \\ 0.473$	$0.422 \\ 0.445$	0.422 0.439	0.371 0.435 0.48 0.461
96 192 336 720	0.375 0.39 0.414 0.42	92	.329 0.299 0.362 0.383 .422 0.431 .442 0.429	$0.402 \\ 0.435$	0.377 0.423	0.398 0.431	$0.381 \\ 0.433$	0.396 0.441	0.372 0.425	0.391 0.432	$0.371 \\ 0.420$	0.389 0.428	0.365 0.415	0.328 0.372 0.417 0.432
送 192 336 720	0.182 0.30 0.349 0.43	08 0.175 0 32 0.306 0	.204 0.089 .304 0.177 .395 0.336 .683 0.851	$0.301 \\ 0.421$	0.174 0.306	0.308 0.397	0.176 0.310	0.311 0.427	0.174 0.305	0.307 0.399	$0.178 \\ 0.307$	0.297 0.399	0.173 0.304	0.201 0.302 0.394 0.685
2 96 192 336 720	0.597 0.36 0.607 0.36	62 0.429 0 69 0.462 0	.288 0.397 .291 0.422 .336 0.437 .323 0.473	$0.278 \\ 0.288$	0.413 0.428	0.269 0.276	$0.515 \\ 0.514$	0.354 0.355	0.427 0.459	$0.281 \\ 0.322$	$0.460 \\ 0.477$	0.273 0.276	0.441 0.454	0.271
Neather 96 192 336 720	0.244 0.27 0.295 0.30	75 0.201 0 99 0.259 0	.191 0.178 .226 0.224 .272 0.281 .332 0.359	$0.259 \\ 0.298$	0.204 0.270	0.241 0.289	$0.228 \\ 0.288$	0.257 0.303	0.202 0.273	$0.239 \\ 0.292$	$0.207 \\ 0.277$	0.242 0.293	0.195 0.243	0.221 0.254

Algorithm 1: CGFM Training

1: **Input:** History distribution p_H , path parameters α_t , β_t , smoothing level σ , network u_t^{θ} , source distribution $p(x_0 \mid h)$, source mode: noise or auxiliary output, prediction objective g_t , and target distribution $q(x_1 \mid h)$.

```
repeat
 2:
             h \sim p_H
 3:
             x_0 \sim p(x_0|h); \ x_1 \sim q(x_1|h)
 4:
 5:
             if source mode == auxiliary output then
 6:
                   \varepsilon \sim \mathcal{N}(0, I)
                   x_0 \leftarrow x_0 + \sigma \varepsilon
 7:
 8:
             end if
             t \sim \mathcal{U}(0,1)
 9:
10:
             x_t \leftarrow \alpha_t x_1 + \beta_t x_0
             \mathcal{L}_{CGM}(\theta) \leftarrow \left\| g_t(x_0, x_1) - u_t^{\theta}(x_t|h) \right\|^2
11:
12:
             \theta \leftarrow \text{Update}(\hat{\theta}, \nabla_{\theta} \mathcal{L}_{CGM}(\theta))
13: until converged
14: Return: u_t^{\theta}
```

Auxiliary Model Enhanced Performance As shown in Table 1, for an input length of 96, the auxiliary model is evaluated across a wide range of mainstream forecasting models, including MLP-based, Transformer-based, and diffusion-based architectures. Our proposed CGFM framework achieves significant performance improvements across most benchmark datasets.

Specifically, CGFM achieves the greatest improvement

when using Rlinear as the auxiliary model, while the gains for iTransformer are comparatively smaller. Notably, iTransformer occasionally exhibits performance degradation; this phenomenon is examined in more detail in Figure 4. As shown on the left of Figure 4, the PCA trajectory of RLinear predictions closely aligns with the ground truth in both shape and continuity, indicating that RLinear effectively captures the temporal evolution of the underlying physical process. In contrast, the middle of Figure 4 shows that iTransformer predictions exhibit an irregular spatial distribution, with discontinuities in inter-point connections. This suggests nonsmooth fluctuations in the high-dimensional representation of iTransformer's predictions. These observations suggest that Transformer architectures are more prone to disrupting the smoothness of the data, thereby posing challenges for learning effective flow paths.

Performance without Auxiliary Model To further validate the superiority of our proposed forecasting framework, we conducted an additional experiment where the initial condition x_0 was directly set as noise under the 96-to-96 prediction setting. CGFM achieved the best overall ranking, demonstrating the effectiveness and soundness of its model architecture. Although it does not attain the best performance on every individual dataset, as shown in Table 1, when combined with an auxiliary model, CGFM consistently achieves the best results across all datasets. This highlights the crucial role of the CGFM auxiliary model in enhancing forecasting perfor-

Table 2: Testing MSE in the multivariate setting. Number in brackets is the rank. CSDI runs out of memory on *Traffic*.

Model	Weather	Traffic	ETTh1	ETTh2	ETTm1	ETTm2	Exchange	Avg Rank
CGFM	0.161(3)	0.430(2)	0.373(1)	0.286(2)	0.317(2)	0.173(2)	0.085(3)	2.142 (1)
TimeDiff	0.181(8)	0.520(7)	0.383(7)	0.301(7)	0.339(8)	0.185(8)	0.087(6)	7.125(7)
CSDI	0.301(13)	= ` ´	0.503(13)	0.356(11)	0.601(13)	0.289(13)	0.258(13)	12.667(13)
iTransformer	0.178(6)	0.397(1)	0.389(10)	0.299(6)	0.336(6)	0.179(6)	0.089(7)	6.000(6)
Rlinear	0.189(9)	0.632(11)	0.382(5)	0.290(4)	0.359(9)	0.182(7)	0.095(8)	7.429(8)
FedFormer	0.219(11)	0.588(8)	0.376(3)	0.359(12)	0.379(11)	0.203(10)	0.147(11)	7.571(9)
TimeMixer	0.165(4)	0.461(4)	0.374(2)	0.294(5)	0.331(5)	0.175(4)	0.083(1)	3.571(4)
TimesNet	0.179(7)	0.593(9)	0.384(9)	0.340(9)	0.338(7)	0.188(9)	0.107(10)	8.571(10)
PatchTST	0.177(5)	0.462(5)	0.383(7)	0.304(8)	0.320(4)	0.175(4)	0.085(3)	5.142(5)
Autoformer	0.266(12)	0.613(10)	0.449(11)	0.345(10)	0.505(12)	0.255(12)	0.189(12)	11.286(12)
TiDE	0.202(10)	0.803(12)	0.478(12)	0.403(13)	0.366(10)	0.209(11)	0.093(8)	10.857(11)
Pathformer	0.156(1)	0.479(6)	0.382(5)	0.283(1)	0.319(3)	0.174(3)	0.083(1)	2.857(3)
MultiPatchFormer	0.158(2)	0.438(2)	0.378(4)	0.285(3)	0.315(1)	0.171(1)	0.085(3)	2.285(2)

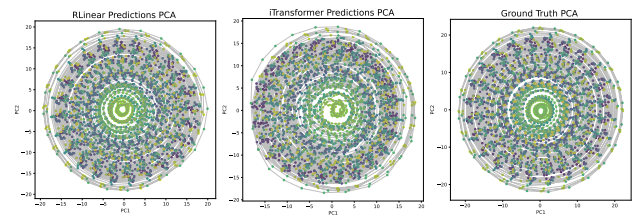


Figure 4: PCA visualization of predictions and ground truth, showing the PCA projections of RLinear predictions, iTransformer predictions, and the ground truth, respectively.

mance.

Case Study of residual learning As shown in Figure 5, we evaluate the 96-to-96 prediction task on the ETTh1 dataset using RLinear as the auxiliary model. The curves represent the mean sequences obtained by averaging all predicted and ground truth windows of length 96. It can be observed that RLinear exhibits persistent underestimation and large variance. In contrast, CGFM effectively learns the residual distribution, substantially reducing both variance and systematic bias, resulting in predictions that closely align with the ground truth.

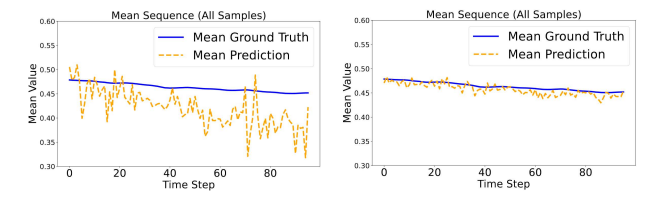


Figure 5: Comparison of results: Left (before CGFM) and Right (after CGFM).

Analysis of Path Hyperparameter We explore different parameterization schemes for affine probabilistic paths, including Optimal Transport (CondOT), Polynomial (Poly-n), Linear Variance Preserving (LinearVP), and Cosine schedulers. Detailed formulas are provided in Appendix.

Table 3 shows that the Poly-n scheduler, with velocity approaching zero near $t \approx 0$, enables thorough exploration around X_0 , similar to the denoising phase in diffusion models. This extension effectively increases the model's decision time, enhancing its ability to capture intricate details early on.

Table 3: MSE and MAE results for different affine conditional paths on ETTh1 and ETTm1 datasets.

Dataset	Con	CondOT		Poly-n		VP		Cosine	
	MSE	MAE	MSE	MAE	MSE	MAE	MSE	MAE	
ETTh1 (Rlinear)	0.368	0.376	0.363	0.372	0.379	0.387	0.380	0.396	
ETTm1 (Rlinear)	0.314	0.363	0.307	0.351	0.336	0.376	0.332	0.371	
ETTh1 (iTrans)	0.374	0.391	0.368	0.388	0.387	0.403	0.387	0.386	
ETTm1 (iTrans)	0.326	0.367	0.313	0.362	0.331	0.372	0.334	0.376	

Table 4: MSE and MAE results for different prediction functions on ETTh1 and ETTm1 datasets.

Dataset	u_t -Pre	diction	X_0 -Pre	ediction	X_1 -Prediction		
	MSE	MAE	MSE	MAE	MSE	MAE	
ETTh1 ETTm1	0.370 0.328	0.379 0.361		0.385 0.367	0.363 0.307	0.372 0.351	

Analysis of Prediction Functions To study different prediction functions' impact on time-series forecasting, we tested ETTh1 and ETTm1 datasets with RLinear as the auxiliary model. Though mathematically equivalent, results (Table 4) show X_1 -Prediction consistently achieves the lowest MSE and MAE, outperforming X_0 - and u_t -Prediction. Intuitively, X_1 -Prediction directly targets the future series, X_0 -Prediction focuses on noise, and u_t -Prediction mixes both. This aligns with prior work (Watson et al. 2023; Shen and Kwok 2023).

Conclusion

In this paper, we propose Conditional Guided Flow Matching (CGFM), a novel model-agnostic framework to enhance time series forecasting. By extending flow matching with auxiliary model outputs, CGFM learns from prediction residuals—structured patterns like systematic biases often overlooked when residuals are treated merely as optimization targets. CGFM incorporates historical data as both conditions and guidance, uses two-sided conditional probability paths, and employs general affine paths to expand the probability path space. These designs avoid path crossing without complex mechanisms, preserve temporal consistency, and strengthen distribution alignment. Extensive experiments show CGFM consistently improves performance and outperforms state-of-the-art models across diverse datasets, validating its effectiveness in advancing time series forecasting

References

- Albergo, M. S.; and Vanden-Eijnden, E. 2023. Building Normalizing Flows with Stochastic Interpolants. arXiv:2209.15571.
- Chen, M.; Peng, H.; Fu, J.; and Ling, H. 2021. Autoformer: Searching transformers for visual recognition. In *Proceedings of the IEEE/CVF international conference on computer vision*, 12270–12280.
- Chen, P.; ZHANG, Y.; Cheng, Y.; Shu, Y.; Wang, Y.; Wen, Q.; Yang, B.; and Guo, C. 2024. Pathformer: Multi-scale Transformers with Adaptive Pathways for Time Series Forecasting. In *The Twelfth International Conference on Learning Representations*.
- Das, A.; Kong, W.; Leach, A.; Mathur, S.; Sen, R.; and Yu, R. 2024. Long-term Forecasting with TiDE: Time-series Dense Encoder. arXiv:2304.08424.
- Esser, P.; Kulal, S.; Blattmann, A.; Entezari, R.; Müller, J.; Saini, H.; Levi, Y.; Lorenz, D.; Sauer, A.; Boesel, F.; Podell, D.; Dockhorn, T.; English, Z.; Lacey, K.; Goodwin, A.; Marek, Y.; and Rombach, R. 2024. Scaling Rectified Flow Transformers for High-Resolution Image Synthesis. arXiv:2403.03206.
- Hu, Y.; Wang, X.; Wu, L.; Zhang, H.; Li, S. Z.; Wang, S.; and Chen, T. 2024. Fm-ts: Flow matching for time series generation.
- Kerrigan, G.; Migliorini, G.; and Smyth, P. 2023. Functional Flow Matching. arXiv:2305.17209.
- Kollovieh, M.; Ansari, A. F.; Bohlke-Schneider, M.; Zschiegner, J.; Wang, H.; and Wang, Y. B. 2024a. Predict, refine, synthesize: Self-guiding diffusion models for probabilistic time series forecasting. *Advances in Neural Information Processing Systems*, 36.
- Kollovieh, M.; Lienen, M.; Lüdke, D.; Schwinn, L.; and Günnemann, S. 2024b. Flow Matching with Gaussian Process Priors for Probabilistic Time Series Forecasting. arXiv:2410.03024.
- Li, Y.; Lu, X.; Wang, Y.; and Dou, D. 2022. Generative time series forecasting with diffusion, denoise, and disentanglement. *Advances in Neural Information Processing Systems*, 35: 23009–23022.
- Li, Z.; Qi, S.; Li, Y.; and Xu, Z. 2023. Revisiting Long-term Time Series Forecasting: An Investigation on Linear Mapping. arXiv:2305.10721.
- Lim, B.; and Zohren, S. 2021. Time-series forecasting with deep learning: a survey. *Philosophical Transactions of the Royal Society A*, 379(2194): 20200209.
- Lipman, Y.; Chen, R. T. Q.; Ben-Hamu, H.; Nickel, M.; and Le, M. 2023. Flow Matching for Generative Modeling. arXiv:2210.02747.
- Liu, X.; Gong, C.; and Liu, Q. 2022. Flow Straight and Fast: Learning to Generate and Transfer Data with Rectified Flow. arXiv:2209.03003.

- Liu, Y.; Hu, T.; Zhang, H.; Wu, H.; Wang, S.; Ma, L.; and Long, M. 2024. iTransformer: Inverted Transformers Are Effective for Time Series Forecasting. In *The Twelfth International Conference on Learning Representations*.
- Naghashi, V.; Boukadoum, M.; and Diallo, A. B. 2025. A multiscale model for multivariate time series forecasting. *Scientific Reports*, 15(1): 1565.
- Nie, Y.; Nguyen, N. H.; Sinthong, P.; and Kalagnanam, J. 2023. A Time Series is Worth 64 Words: Long-term Forecasting with Transformers. arXiv:2211.14730.
- Shen, L.; Chen, W.; and Kwok, J. 2024. Multi-Resolution Diffusion Models for Time Series Forecasting. In *The Twelfth International Conference on Learning Representations*.
- Shen, L.; and Kwok, J. 2023. Non-autoregressive conditional diffusion models for time series prediction. In *International Conference on Machine Learning*, 31016–31029. PMLR.
- Tamir, E.; Laabid, N.; Heinonen, M.; Garg, V.; and Solin, A. 2024. Conditional Flow Matching for Time Series Modelling. In *ICML 2024 Workshop on Structured Probabilistic Inference & Generative Modeling*.
- Tashiro, Y.; Song, J.; Song, Y.; and Ermon, S. 2021. Csdi: Conditional score-based diffusion models for probabilistic time series imputation. *Advances in Neural Information Processing Systems*, 34: 24804–24816.
- Tong, A.; Fatras, K.; Malkin, N.; Huguet, G.; Zhang, Y.; Rector-Brooks, J.; Wolf, G.; and Bengio, Y. 2024. Improving and generalizing flow-based generative models with minibatch optimal transport. arXiv:2302.00482.
- Wang, S.; Wu, H.; Shi, X.; Hu, T.; Luo, H.; Ma, L.; Zhang, J. Y.; and Zhou, J. 2024. Timemixer: Decomposable multiscale mixing for time series forecasting. *arXiv* preprint *arXiv*:2405.14616.
- Watson, J. L.; Juergens, D.; Bennett, N. R.; Trippe, B. L.; Yim, J.; Eisenach, H. E.; Ahern, W.; Borst, A. J.; Ragotte, R. J.; Milles, L. F.; et al. 2023. De novo design of protein structure and function with RFdiffusion. *Nature*, 620(7976): 1089–1100.
- Wu, H.; Hu, T.; Liu, Y.; Zhou, H.; Wang, J.; and Long, M. 2022. Timesnet: Temporal 2d-variation modeling for general time series analysis. *arXiv* preprint arXiv:2210.02186.
- Yoon, J.; Jarrett, D.; and Van der Schaar, M. 2019. Timeseries generative adversarial networks. *Advances in neural information processing systems*, 32.
- Zhang, X. N.; Pu, Y.; Kawamura, Y.; Loza, A.; Bengio, Y.; Shung, D.; and Tong, A. 2024. Trajectory flow matching with applications to clinical time series modelling. *Advances in Neural Information Processing Systems*, 37: 107198–107224.
- Zhou, T.; Ma, Z.; Wen, Q.; Wang, X.; Sun, L.; and Jin, R. 2022. Fedformer: Frequency enhanced decomposed transformer for long-term series forecasting. In *International conference on machine learning*, 27268–27286. PMLR.